

Supporting Information

# **A Smartphone-Enabled Portable Digital Light Processing 3D Printer**

*Wanlu Li<sup>‡</sup>, Mian Wang<sup>‡</sup>, Luis Santiago Mille, Juan Antonio Robledo, Valentín Huerta, Tlalli Uribe, Feng Cheng, Hongbin Li, Jiaxing Gong, Terry Ching, Caroline A. Murphy, Ami Lesha, Shabir Hassan, Tim Woodfield, Khoon S. Lim\*, Yu Shrike Zhang\**

W. Li, Dr. M. Wang, L. Mille, A. Robledo, V. Huerta, T. Uribe, F. Cheng, H. Li, J. Gong, T. Ching,  
A. Lesha, Dr. S. Hassan, Prof. Y. S. Zhang

Division of Engineering Medicine, Department of Medicine, Brigham and Women's Hospital,  
Harvard Medical School, Cambridge, MA 02139, USA

\*E-mail: [yszhang@research.bwh.harvard.edu](mailto:yszhang@research.bwh.harvard.edu)

Dr. C. A. Murphy, Prof. T. Woodfield, Dr. K. S. Lim

Christchurch Regenerative Medicine and Tissue Engineering (CReaTE) Group, Department of  
Orthopaedics Surgery and Musculoskeletal Medicine, University of Otago Christchurch,  
Christchurch 8011, New Zealand

\*E-mail: [khoon.lim@otago.ac.nz](mailto:khoon.lim@otago.ac.nz)

<sup>‡</sup>Wanlu Li and Mian Wang contributed equally to this work

## Experimental

**Hardware assembly of the smartphone-enabled DLP printer:** Three different black acrylic platforms were used to support the mirror, the optical lens, and the vat, which were mounted on carbon steel guide rods to ensure the stability and stiffness of the whole structure. The developed device used a commercially available Nema 11 stepper motor to control the Z-axis position of the build platform. This was based on the transformation of the rotational motion of the motor into a linear way by using a 100-mm linear rail with a T6 × 1 lead screw (single start, 1 mm between peaks). Besides, a stepper motor driver with a 1/8 micro-stepping configuration provided a moving distance of 5 μm per step to the build platform. The structure also supported a limit switch used to restrict the platform travel and help standardize and define a Z-axis starting point for the printing process. Considering the printed structure is attached to the build platform after every printing, the build platform was designed as removable from the device so that the user can easily take the printed object out without breaking it. The build platform was made with poly(lactic acid) (PLA, Hatchbox3d) and coated with a circular cover glass (15 mm, Carolina) as the surface of the build platform, achieving a strong material attachment due to the hydrophilicity and smoothness of the glass. An MG90s servomotor served to control a physical light block to stop the light when the printing process was completed. Overall, the whole structure was screwed to an acrylic base to fix it. An acrylic case was designed to protect all the components, isolate the optical system and the vat from the environmental light. PLA structures were printed using a fused deposition modeling 3D printer (Flashforge Creator PRO), whereas the acrylic pieces were fabricated using a laser cutter (Desktop Laser VLS 2.30, Universal Laser Systems). Models of PLA and acrylic

components were designed with SolidWorks.

**Optical components and magnification calculations:** To perform a mathematical analysis of the optical system, the projector was placed in front of a projection screen 371.6 mm (image distance,  $d_{i1}$ ) from the projector lens to the screen. The projected image height was then measured, giving 234 mm, and compared to the original size of the LCD screen used in the projector, which was 6.5 mm. By doing so, the magnification between LCD screen and projection screen ( $M_1$ ) was obtained, resulting in  $M_1 = -36$ . Using **Equation 2**,  $M_1$ , and  $d_{i1}$ , it was possible to calculate the distance from the LCD screen to the projector lens (object distance,  $d_{o1}$ ), resulting in 10.32 mm. Using **Equation 3**, the focal length of the lens in the projector ( $f_1$ ) was calculated, giving  $f_1 = 10.06$  mm.

$$M = \frac{d_i}{d_o} \quad (2)$$

$$\frac{1}{f} = \frac{1}{d_o} + \frac{1}{d_i} \quad (3)$$

As the two lenses (projector lens and the lens we added) interacted in the system, it was necessary to picture the system and understand how these two interacted correctly. **Figure 1cii-ciii** shows a diagram of the system to make this clear. For the first lens (projector lens), the focal length ( $f_1 = \sim 10$  mm), the distances ( $d_{i1} = 371.6$  mm,  $d_{o1} = 10.32$  mm), and the magnification ( $M_1 = -36$ ) were already calculated above. By looking at the diagram, it can be noticed that  $d_{i1}$  goes beyond the second lens, which will cause the  $d_{o2}$  to be negative. Apart from that, the distance between the two lenses has to be added; as this distance is positive, the object distance for the second lens is  $d_{o2} = -267.6$  mm. Having  $d_{o2}$ , the second focal length ( $f_2 = 10$  cm), and **Equation 3**, the final image distance is  $d_{i2} = 72.8$  mm. Finally, the second magnification between the lens we added and vat is

$M_2 = 0.2720$ . The final magnification of the system is calculated by multiplying both magnifications, resulting in  $M = -9.79$ . It indicated that patterns were approximately 10 times smaller after focused by the optical system.

**Programming principle of the smartphone printing App:** Android OS supports Bluetooth protocol stack, which enables the wireless exchange of data with other Bluetooth devices. The programming language chosen to develop the mobile application was Python, which has many libraries for scientific computing to construct a simple and powerful system. Additionally, the App was developed in Python using Kivy, an open-source Python library for developing mobile applications, and NumPy as a general-purpose array-processing package for scientific computing. PyJNIus was used to access Java classes as Python classes. Of note, a similarly functioning iOS App is feasible as well, which however was not developed given the scope of the current work.

**Synthesis of GelMA and GelAGE:** GelMA was synthesized from gelatin of cold-water fish skin based on methods reported previously.<sup>[32]</sup> Fish gelatin has a lower melting point than porcine gelatin, which is suited for DLP printing at room temperature.<sup>[33]</sup> Gelatin (Sigma-Aldrich) dissolved in phosphate-buffered saline (PBS, Thermo Fisher, 10 w/v%) at 50 °C was reacted with methacrylic anhydride (Sigma-Aldrich, gelatin:methacrylic anhydride = 10 g:8 mL) at 50 °C for 1 h. After dialyzing with the dialysis membrane ( $M_w$  cut-off = 14 kDa, Spectrum) against deionized water at 40 °C for 5 days, it was lyophilized with a freeze-dryer (Alpha 1-2 LDplus, Christ) and stored at -20 °C until use. The synthesis of GelAGE was conducted as reported previously.<sup>[34]</sup>

Gelatin was dissolved in deionized water (10 w/v%) at 65 °C, and it was reacted with 12 mmol of allyl glycidyl ether (AGE, Sigma-Aldrich) and 2 mmol of sodium hydroxide (NaOH, Sigma-Aldrich) for 8 h at 65 °C. After dialyzing ( $M_w$  cut-off = 1 kDa) against deionized water, it was lyophilized and stored at 4 °C until use.

**Preparation of PEGDA, GelMA, and GelAGE inks:** PEGDA ( $M_w = 575$  Da, Sigma-Aldrich) was diluted in PBS to a concentration of 40 v/v%. PBS was used to dissolve the lyophilized GelMA into 20 w/v% of concentration and then mixed with 4-arm PEG-acrylate power (1 w/v%,  $M_w = 10,000$  Da, JenKem). GelAGE was also dissolved in PBS at a 20 w/v% concentration and mixed with DTT (120 mM, Sigma-Aldrich). Additionally, 2-mM/20-mM Ru/SPS was added as the photoinitiator, and 0.5 wt.% to 2.5 wt.% photoabsorber (Ponceau 4R, Sigma-Aldrich) was blended into the inks before the printing.

**Printability Evaluation of PEGDA inks:** Photoinitiator (2-mM/20-mM Ru/SPS or 4-mM/40-mM Ru/SPS) and photoabsorber (0.5 wt.% or 1.0 wt.% of Ponceau 4R) were added to PEGDA ( $M_w = 575$  Da) inks of 20 v/v%, 40 v/v%, and 60 v/v% of concentrations. Square patterns with side lengths ranging from 150, 300, 400, to 600  $\mu\text{m}$  were printed to assess the printability of printed planar constructs. Exposure time was varied from 10 to 60 s. We used printing ratio, which was defined as the ratio of the printed size to the designed size, to analyze the result of printability. Printing ratio equal to 0 was identified as non-printable, higher than 0 but below 1 as partially printable, and a value of 1 as printable.

**Preparation of the bioink for in situ printing:** C2C12 cells (ATCC) were suspended in 10 w/v% GelMA at a density of  $8 \times 10^6$  cells mL<sup>-1</sup>, and 2-mM/20-mM Ru/SPS was added as the photoinitiator. The bioink was printed immediately after preparation and thoroughly mixed before printing to avoid cell aggregation and sedimentation.

**Cell viability analysis of C2C12 cells:** The live/dead staining was performed on day 1, day 3, day 7, and day 14, as previously reported.<sup>[32b]</sup> The samples were rinsed with PBS, and then they were incubated with the staining solution (2- $\mu$ M calcein-AM and 4- $\mu$ M ethidium homodimer-1, Thermo Fisher) for 30 min at 37 °C. The constructs were visualized with an inverted fluorescence microscope (Eclipse Ti, Nikon).

**Scanning 3D objects using the smartphone App Qlone:** For scanning with the Qlone App, the intended object was placed in the middle of the template mat that contained a set of black/white grids to ordinate it. Subsequently, the augmented reality (AR) dome presented on the smartphone screen guided to take the video of the object from all angles. Additionally, models built by different poses of the same object could be merged to promote the scanning accuracy after processing in the App. The scanned models were exported in the STL format for slicing and 3D printing using our customized printing App on the same smartphone.

**Statistical analyses:** Data are presented as the means  $\pm$  standard deviations (SDs). All statistical

analysis was performed with one-way analysis of variance (ANOVA) followed by two-tailed Student's *t*-test or Tukey's Honest Significant Difference test. Data were presented at 95% confidence interval, and  $p < 0.05$  was considered statistically significant.

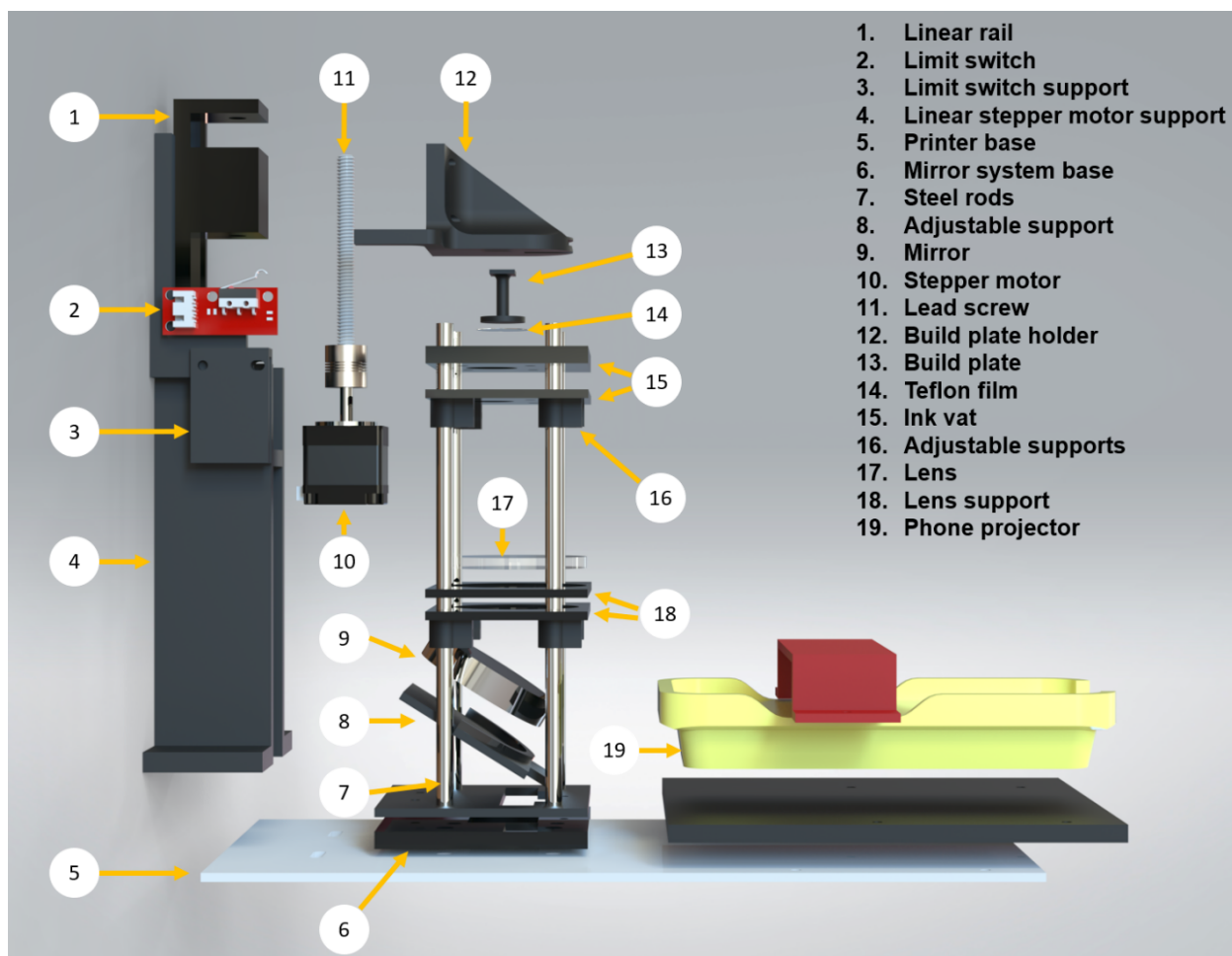


**Figure S1.** Hardware assembly of the smartphone-enabled DLP printer.



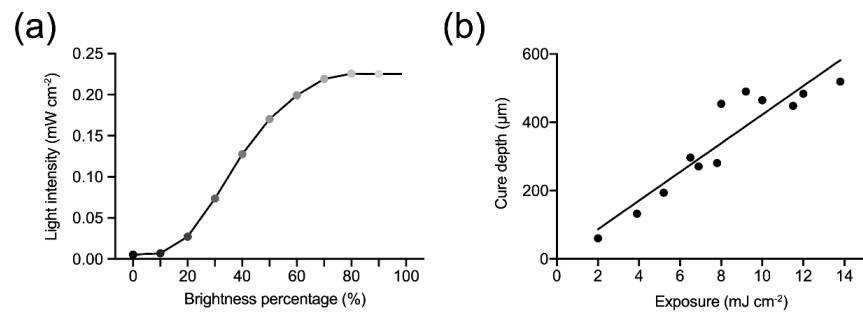


**Figure S2.** Light feature of the smartphone-enabled DLP printer. (a) Light density conversion of projector brightness. (b) Working curve of the 40 v/v% PEGDA ( $M_w = 575$  Da) ink.

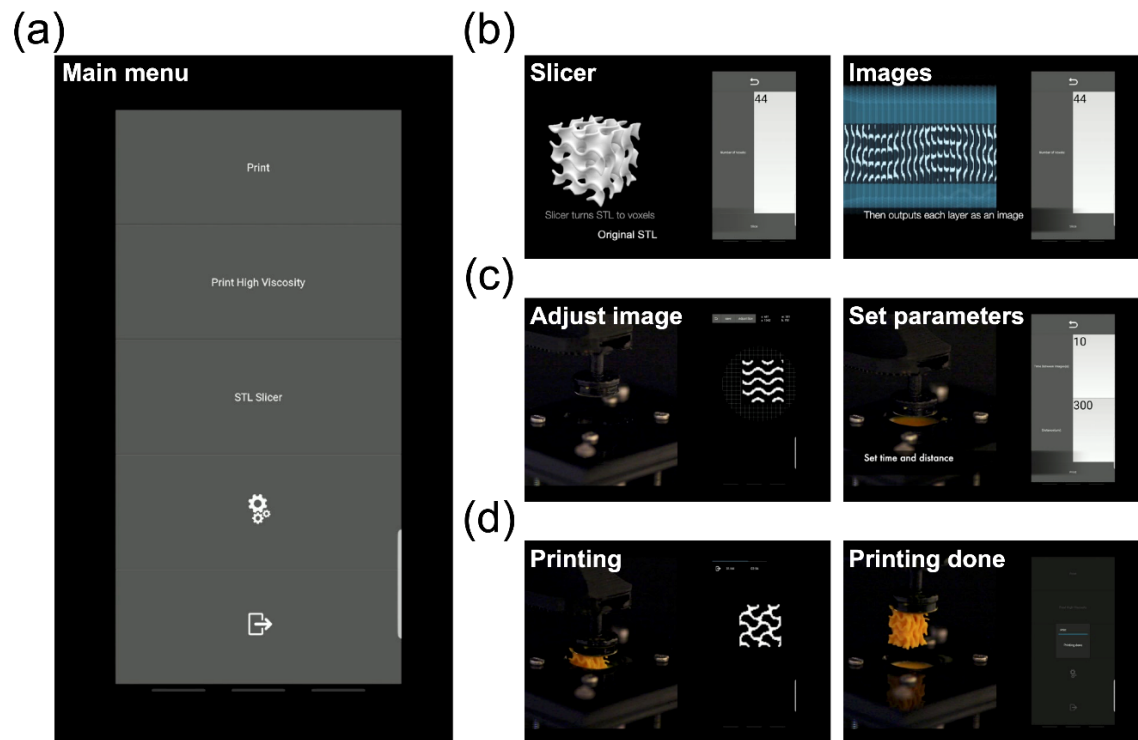


**Figure S3.** Screenshots of the printing App. (a) Main menu shows functions of the printing App, including 3D model-slicing, parameter-setting, and printing. (b) Slicing with customizable voxel numbers, and images presenting on the App after slicing. (c) Adjusting the image size and position, and setting printing time and distance for each layer. (d) Printing layer number and remaining time are presented during the printing process.

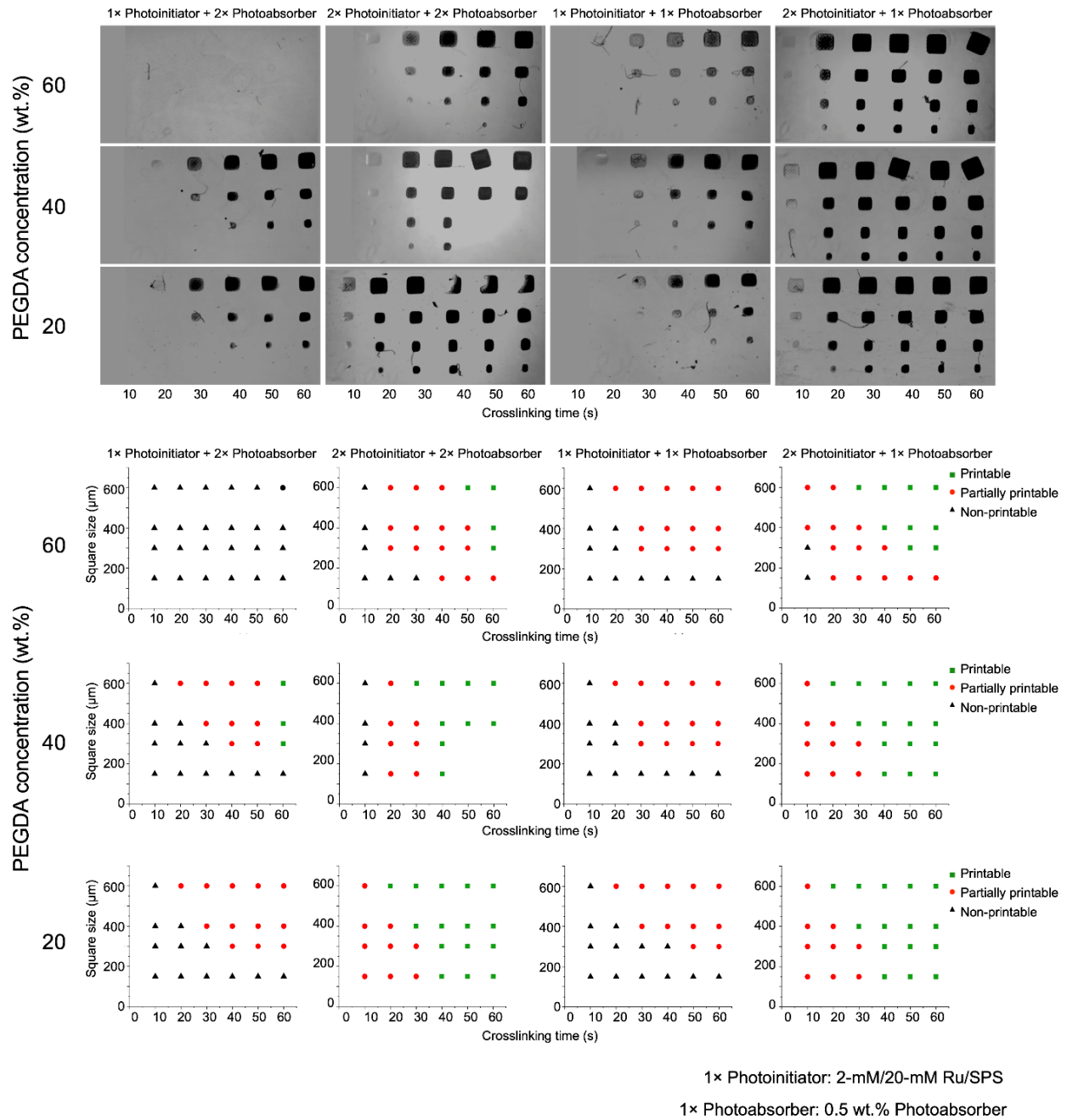


**Figure S4.** Printability of PEGDA ( $M_w = 575$  Da) with photoabsorber under different crosslinking times when exposed to square patterns with side lengths ranging from 150, 300, 400, to 600  $\mu\text{m}$ .

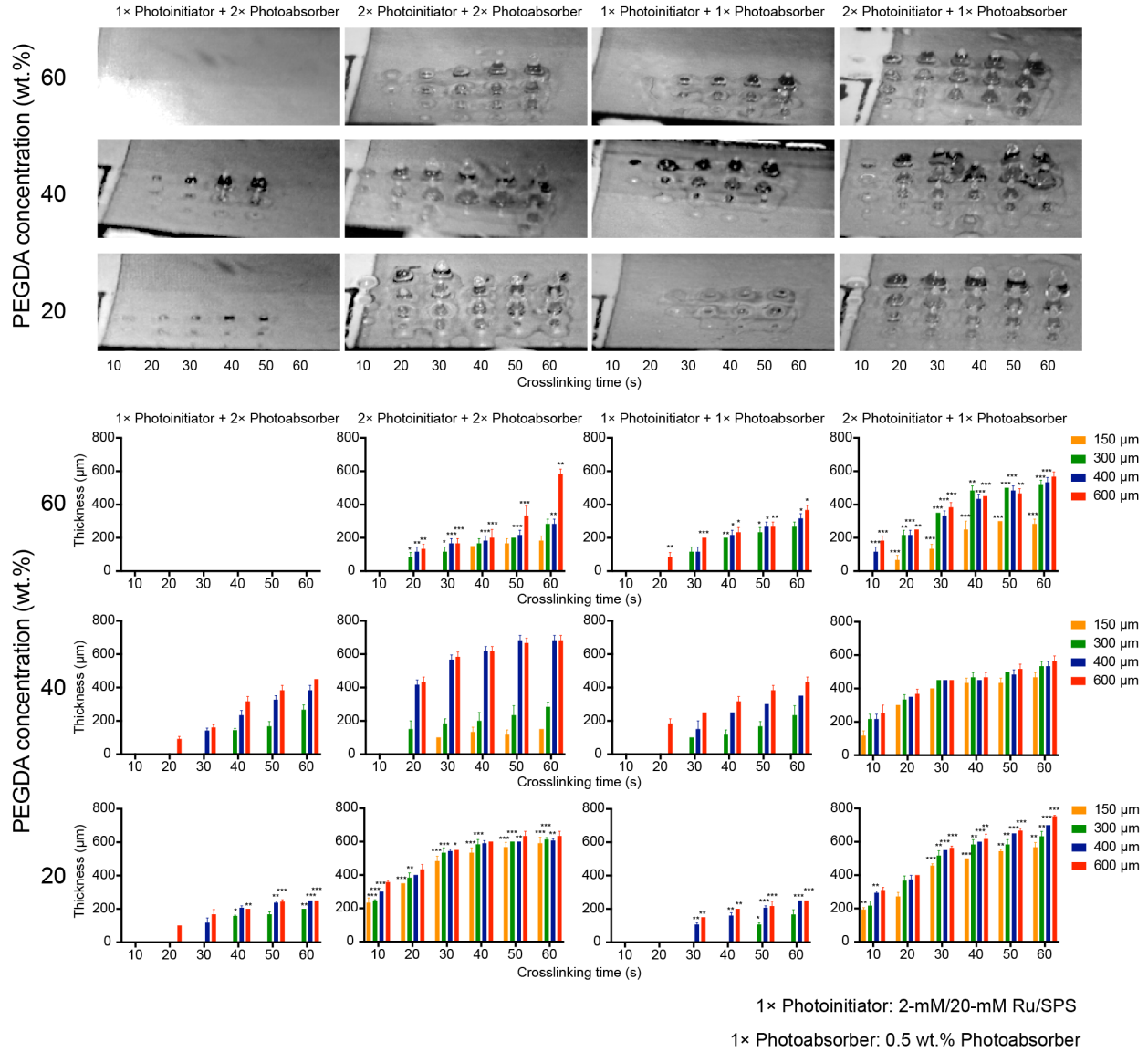
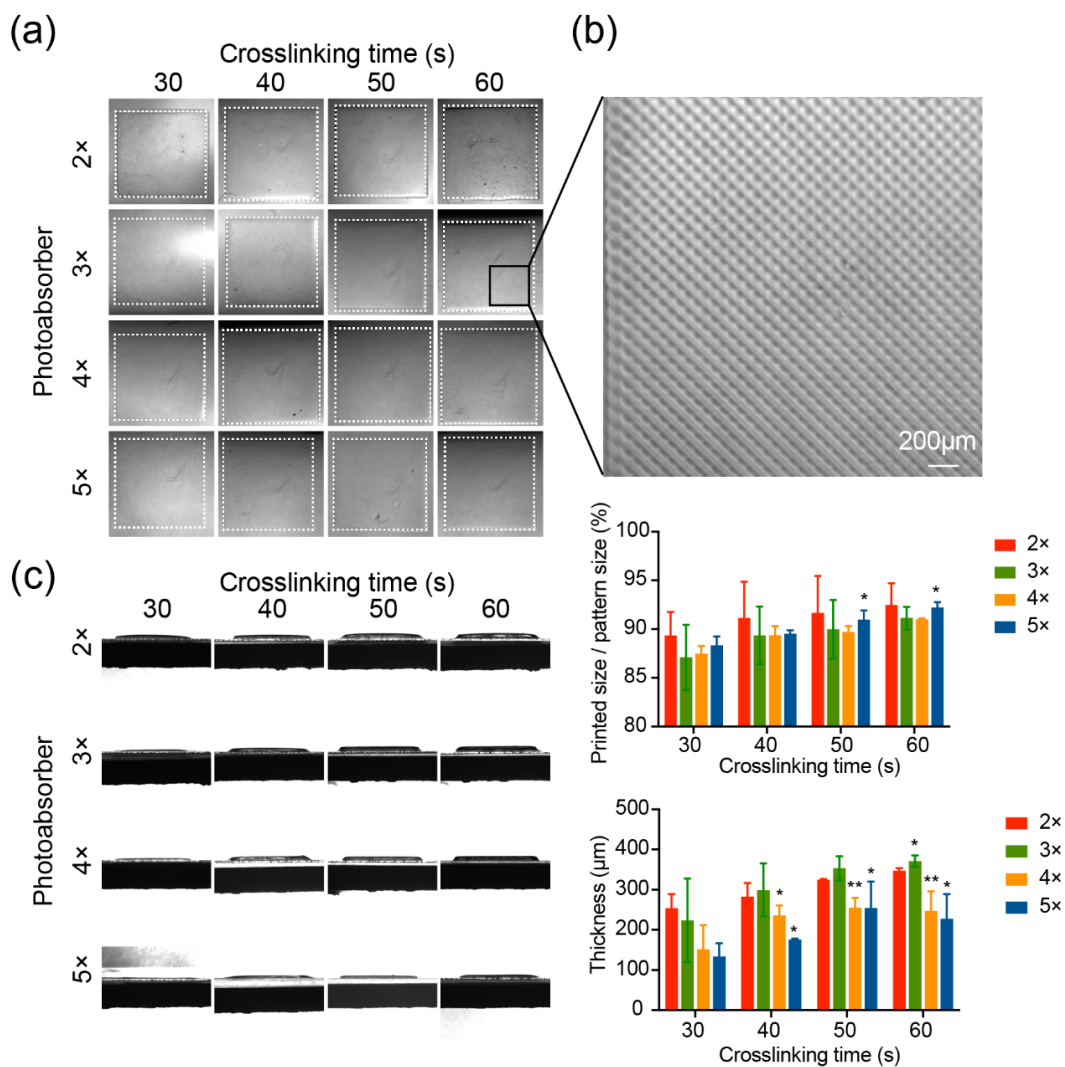


**Figure S5.** Crosslinking thickness of PEGDA ( $M_w = 575$  Da) with photoabsorber under different crosslinking times when exposed to square patterns with side lengths ranging from 150, 300, 400, to 600  $\mu\text{m}$ . \* $P < 0.05$ , \*\* $P < 0.01$ , \*\*\* $P < 0.001$ ; one-way ANOVA (compared with the corresponding thickness achieved by 40 v/v% PEGDA); means  $\pm$  SDs ( $n = 3$ ).



1× Photoabsorber: 0.5 wt.% Photoabsorber

**Figure S6.** Printing fidelity of 40 v/v% PEGDA ( $M_w = 575$  Da) containing 2-mM/20-mM Ru/SPS with photoabsorber under different crosslinking times. Photopolymerization (a) size and (c) thickness at different crosslinking times with different concentrations of photoabsorber. (b) Enlarged image from the black square in (a) showing the pixel size in the printing area. \* $P < 0.05$ , \*\* $P < 0.01$ ; one-way ANOVA (compared with size ratio or thickness achieved by inks containing 2× photoabsorber); means  $\pm$  SDs ( $n = 3$ ).

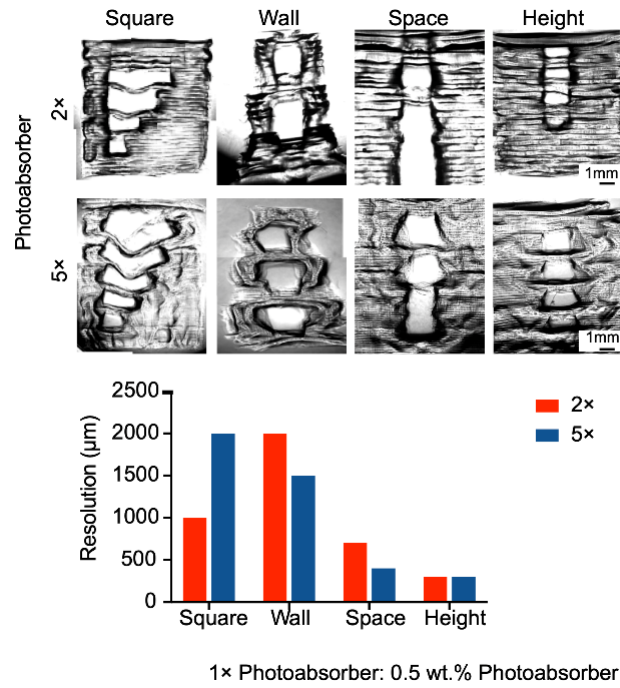


**Figure S7.** Axial resolution characterizations of the printed constructs with internal cavities, including the longest square, thinnest wall, smallest space, and minimum square height.

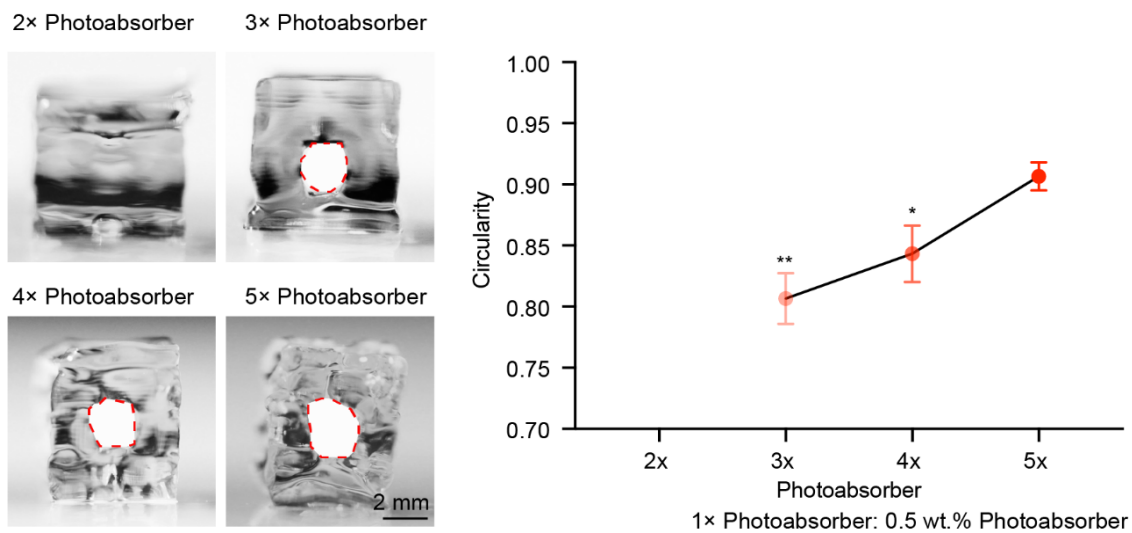


**Figure S8.** Circularity of printed channels with different concentrations of photoabsorber. \* $P < 0.05$ , \*\* $P < 0.01$ ; one-way ANOVA (compared with circularity achieved by ink containing 5× photoabsorber); means  $\pm$  SDs ( $n = 3$ ).

**Moai SLA 3D Printer**                      **Smartphone-DLP**  
**(Peopoly Moai Tough Resin)**            **(Photocentric Daylight Firm Resin)**



**Figure S9.** Comparison of Shanghai Oriental Pearl Towers printed by the commercial SLA printer and the smartphone-enabled DLP.





**Movie S1.** Gyroid printing using the smartphone-enabled DLP printing system (played back at 4X speed).

**Movie S2.** Dye perfusion of a helix channel printed with 40 v/v% PEGDA ( $M_w = 575$  Da), 2-mM/20-mM Ru/SPS, and 2.5 wt.% Ponceau 4R (played back in real time).